07

Bimodal Whispering-Gallery Mode Lasing in Micropillar Cavity Lasers

© A.V. Babichev[1], I.S. Makhov[2], N.V. Kryzhanovskaya[2], Yu.M. Zadiranov[1], Yu.A. Salii[1], M.M. Kulagina[1], Ya.N. Kovach[1,3], M.A. Bobrov[1], A.P. Vasiliev[1], S.A. Blokhin[1], N.A. Maleev[1], L.Ya. Karachinsky[3], I.I. Novikov[3], A.Yu. Egorov[3]

[1] Ioffe Institute, St. Petersburg, Russia
[2] HSE University, St. Petersburg, Russia
[3] ITMO University, St. Petersburg, Russia
E-mail: a.babichev@mail.ioffe.ru

Received September 23, 2024
Revised October 28, 2024
Accepted November 5, 2024

The results of the study of whispering-gallery mode splitting in lasers of the spectral range of 930−950 nm based on a vertical microcavity are presented. The use of non-absorbing distributed Bragg reflectors based on alternating $Al_{0.2}Ga_{0.8}As/Al_{0.9}Ga_{0.1}As$ layers, made it possible to reduce the threshold optical pump power to 180 μW (for a 3 μm micropillar cavity laser). The bare quality factor for whispering-gallery modes exceeded 14 000. A significant energy distance between the modes ($\sim$ 80 μeV), along with high stability of the lasing wavelength with increasing pump level ($\sim$ 220 μeV), indicates the prospects for using these lasers to modulate the polarization of radiation.

Keywords: quantum dots, molecular-beam epitaxy, Stransky−Krastanov mechanism, gallium arsenide, birefringence, bimodality.

DOI: 10.61011/TPL.2025.03.60716.20129

Vertically-emitting lasers (VEL) are the key element of high-speed optical connections. The limiting frequency of small-signal modulation of the signal amplitude in VEL is 40 GHz [1].

The concept based on the development of bimodal lasers [2–5] enables to increase the frequency of low-signal modulation of spin VELs up to 200 GHz by modulating the radiation polarization [2].

The main advantages of microlasers with optical pumping based on vertical microcavities compared to VELs are a significant decrease in the threshold pumping power and the possibility of creating denser laser arrays. The first results on implementing the modulation of radiation polarization in bimodal microlasers are given in [6]. The authors managed to implement the frequency of small-signal polarization modulation $\sim$ 10 GHz in microlasers with a threshold pumping power of 2.1 mW [6], where due to the ellipticity of the microcavity in the cross section [7,8] the value of mode splitting was $\sim$ 41 μeV.

In this paper we present the first results on implementing bimodal generation on whispering gallery modes (WGM) in lasers with a vertical microcavity.

The heterostructure was grown by molecular-beam epitaxy on a semi-insulating GaAs substrate with $(100) \pm 0.5^\circ$crystal-lattice orientation. The bottom and top distributed Bragg reflectors included 35 and 27 pairs of alternating quarter-wave $Al_{0.2}Ga_{0.8}As/Al_{0.9}Ga_{0.1}As$ layers. The vertical microcavity was formed based on 210 nm-thick GaAs, in the center of which three layers of InGaAs quantum dots (QDs) separated by 20 nm-thick GaAs layers were placed. The self-organization of the QDs occurred by the Stranski−Krastanov mechanism from a layer of $In_{0.5}Ga_{0.5}As$ with a thickness of 5.5 monolayers.

The heterostructure was etched by dry ion etching through a photoresist-based mask. The microlaser diameters measured in orthogonal directions were 3.13 and 3.15 μm corresponding to an ellipticity of ε [6], equal to 0.4 %.

Optical measurements were performed in a Montana Instruments Cryostation s50 closed-loop cryostat. The microlaser was pumped through an upper distributed Bragg reflector by a semiconductor laser with a generation wavelength of 808 nm in continuous mode. The pump laser radiation was focused using a Mitutoyo MPlan Apo NIR micro lens with 50-x magnification. The size of the pumping spot corresponded to the diameter of the microlaser. An Andor Shamrock 500i monochromator with a DU 401A BVF cooled silicon CCD matrix was used to record the radiation. The use of a diffraction grating with 1200 at 1 mm grooves provided a spectral resolution of 0.05 nm. The microphotoluminescence spectra were measured at 77 K.

As the optical pumping power increases, a superlinear increase in the integrated intensity for the two luminescence lines (at wavelengths 930 and 951 nm) is observed, which, along with the narrowing of the half-width of the lines, indicates a transition to laser generation [9]. The intermode spacing (FSR), equal to $\sim$ 30 meV, corresponds to the case of generation at WGM and is described using the expression [10–12]: $\mathrm{FSR} = hc/\pi D n_{eff}$, where h — Planck constant, c — the speed of light in vacuum, D — the diameter of the microlaser, and n_{eff} — the effective refractive index. Value n_{eff} is evaluated using the expression [10,12]: $n_{eff} = 3.693 - 1.052E + 0.610E^2$, where E — the quantum energy for TE-modes observed at WGM-generation in QD

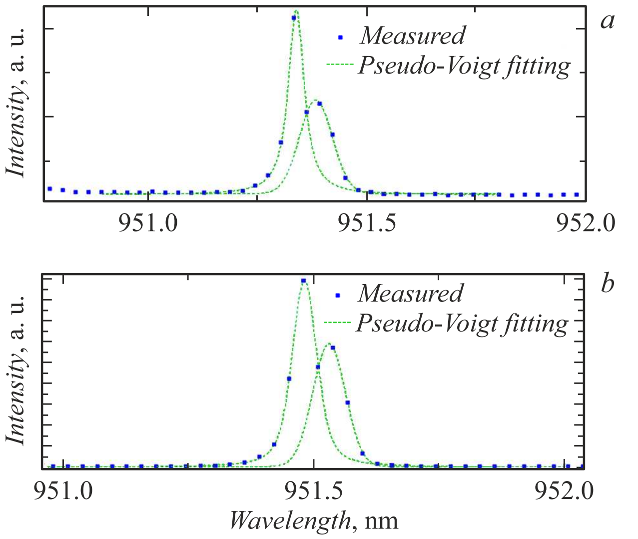

Figure 1. Generation spectra at 183 μW (a) and 1.65 mW (b) optical pumping powers with the approximation result (dashed lines) for each peak (based on the pseudo-Voit [9,14]).

microlasers [10]. Over the whole range of pumping levels, generation at two WGM is observed, which is due to the small value of the mismatch between the position of the resonant wavelength of the microcavity and the position of the maximum of the QD photoluminescence spectrum (gain to cavity detuning, GCD) [13]. The GCD value obtained from the analysis of the QD photoluminescence spectra measured from the end of the heterostructure was 12 meV. The azimuthal mode order was estimated based on the expression $m = \pi D n_{eff}/\lambda$, where λ — generation wavelength. It is shown that the WGM lines with generation wavelengths of 930 and 951 nm correspond to generation in the 36th and 35th modes. For both modes, a splitting of the generation line into two components is observed (Fig. 1).

The weak S-shaped dependence of the integrated luminescence intensity on the optical pump level for two lines near 951 nm, typical for laser generation with a high value of the spontaneous emission fraction in the microcavity [9] mode, is shown in Fig. 2, a. An approximation of the data based on the$n(P_{pump})$ dependence was performed, with the inverse dependence of the pumping power P_{pump} on the average exciton number$n$ determined using the expression [12,15]: $P_{pump} = \Gamma n\big(1 + 2\xi + 2\beta(n - \xi)\big)/\beta(1 + 2n)$, where ξ — the average number of excitons corresponding to the transparency threshold, β — he fraction of spontaneous emission in the microcavity mode (β-factor). Value $\xi' = \xi/\beta$ is determined based on a two-level model [16,17]: $\xi' = N/2 \cdot \tau\Gamma$, where N — the number of QDs in a microlaser of a given diameter τ — the radiative recombination time. The value of the weighting factor Γ is determined using the expression [15]: $\Gamma = A \cdot 2\pi\Delta E(1 + 2n)/\big(h(1 + 2\xi)\big)$, where ΔE — the half-width of the generation line, A — the weighting factor between the pumping rate and P_{pump}. The model curves correspond to a β-factor equal to 0.9 %. The estimated threshold power of $P_{th} = \Gamma\big(1 + 2\xi + 2\beta(1 - \xi)\big)/3\beta$ was $\sim 180\,\mu$W. This value is comparable to the previously reported results for microlasers with generation on WGM

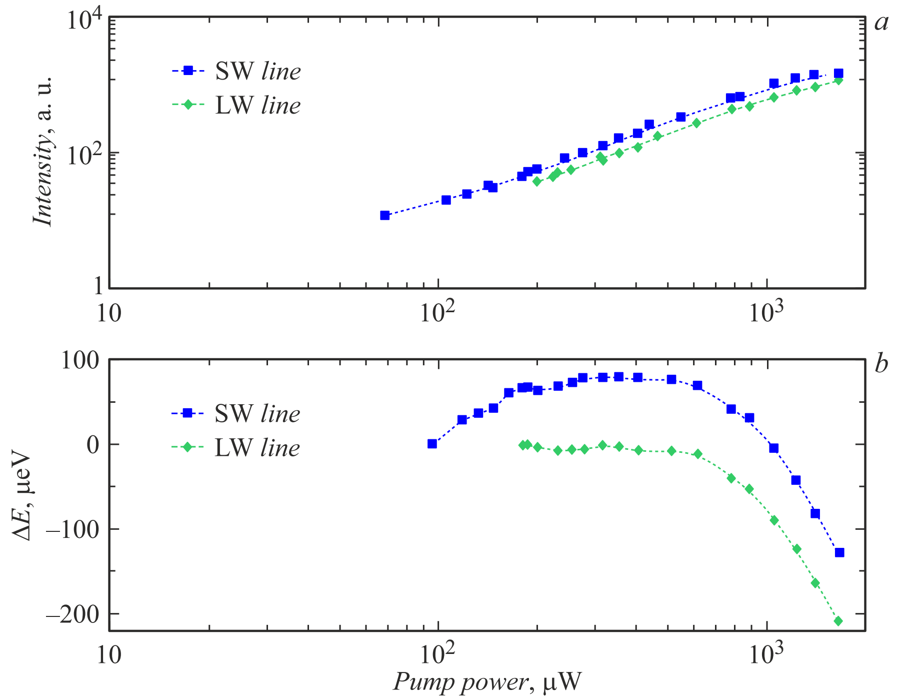

Figure 2. a — the dependence of the integrated emission intensity on the optical pumping power for modes with generation wavelengths of 951.34 nm (SW *line*) and 951.39 nm (LW *line*). b — the spectral shift of the position of the short-wave (SW *line*) and long-wave (LW *line*) modes with increasing optical pumping level.

but pumped through the side surface of the microcavity ($P_{th} = 235\,\mu$W at 20 K [18]). The finesse value of the Q, microcavity measured at the laser generation threshold (bare Q-factor), was 16 000 and 14 000 for the shortwave and longwave modes. Further increasing the optical pumping level increased the microcavity finesse to at least 20 000 (limited by the spectral resolution of the monochromator).

The spectral shift of the mode position ΔE) value) as the optical pumping level increased, was evaluated (Fig. 2, *b*). At low pumping level, a short-wavelength shift in the position of generation lines is observed due to an increase in the number of free charge carriers, the concentration of which is proportional to the optical pumping power [9]. When the optical pumping level exceeds $400\,\mu$W a long-wavelength shift in the position of the generation lines is observed, indicating the predominance of the contribution due to thermal effects [9]. Exceeding the pumping threshold level by a factor of 10 (~ 1.8 mW) results in a shift of the generation line position by an amount of about $220\,\mu$eV. Figure 2, *b* shows that the magnitude of the WGM splitting was $67\,\mu$eV near the generation threshold and $80\,\mu$eV at $10P_{th}$. Previously, the maximum value of the splitting in a $3\,\mu$m-microlaser with generation on the vertical mode did not exceed $70\,\mu$eV [6] and corresponded to the ellipticity of the microcavity equal to 10%.

Thus, the paper presents the first results on implementation of bimodal generation on whispering gallery modes in lasers with a vertical microcavity. The use of mirrors that do not absorb at the pump wavelength allowed reducing the threshold pumping power to $180\,\mu$W, more than 10 times compared to microlasers with vertical mode splitting due to the microcavity ellipticity [6]. The reduction of the laser thermal load allowed implementing an ultra-small shift of the generation wavelength as the pumping level increases ($220\,\mu$eV at $10P_{th}$), which correlates with the previously presented results for the case of vertical mode generation ($250\,\mu$eV at $10P_{th}$ [9]) in microlasers with non-absorbing mirrors. The intermode distance at different pumping levels is evaluated. It is shown that the maximum WGM splitting is of the order of $80\,\mu$eV, which corresponds to a frequency difference of bimodal generation lines of 20 GHz. Further studies will be aimed at investigating the polarization dynamics in spin lasers based on the formed vertical microcavities.

Funding

The work by the authors from the Ioffe Institute of Physics and Technology was supported by the grant of the Russian Science Foundation № 22-19-00221 (https://rscf.ru/project/22-19-00221/) in terms of design development, heterostructure epitaxy, microlaser formation, and generation spectra measurement. I.S. Makhov, N.V. Kryzhanovskaya would like to thank the Fundamental Research Program of the National Research University Higher School of Economics for the support in the study of photoluminescence spectra from a microcavity heterostructure chip (at the angle of 90°).

Conflict of interest

The authors declare that they have no conflict of interest.

References

[1] A. Liu, P. Wolf, J.A. Lott, D. Bimberg, Photon. Res., **7** (2), 121 (2019). DOI: 10.1364/prj.7.000121
[2] M. Lindemann, G. Xu, T. Pusch, R. Michalzik, M.R. Hofmann, I. Žutić, N.C. Gerhardt, Nature, **568** (7751), 212 (2019). DOI: 10.1038/s41586-019-1073-y
[3] K. Panajotov, Opt. Lett., **49** (13), 3789 (2024). DOI: 10.1364/ol.531094
[4] M. Zou, X.-H. Jia, W.-J. Song, S.-S. Deng, M.-Y. Bao, Y.-Q. Tang, J.-T. Lv, X.-Y. Li, X. Zhang, Jpn. J. Appl. Phys., **63** (9), 092004 (2024). DOI: 10.35848/1347-4065/ad7791
[5] S. Guessoum, A. Kyriazis, T. Malica, J. Van Erps, G. Van Steenberge, M. Virte, Opt. Lett., **49** (15), 4477 (2024). DOI: 10.1364/ol.532942
[6] N. Heermeier, T. Heuser, J. Große, N. Jung, A. Kaganskiy, M. Lindemann, N.C. Gerhardt, M.R. Hofmann, S. Reitzenstein, Laser Photon. Rev., **16** (4), 2100585 (2022). DOI: 10.1002/lpor.202100585
[7] S. Ates, S.M. Ulrich, P. Michler, S. Reitzenstein, A. Löffler, A. Forchel, Appl. Phys. Lett., **90** (16), 161111 (2007), DOI: 10.1063/1.2724908
[8] D.M. Whittaker, P.S.S. Guimaraes, D. Sanvitto, H. Vinck, S. Lam, A. Daraei, J.A. Timpson, A.M. Fox, M.S. Skolnick, Y.-L.D. Ho, J.G. Rarity, M. Hopkinson, A. Tahraoui, Appl. Phys. Lett., **90** (16), 161105 (2007). DOI: 10.1063/1.2722683
[9] C.-W. Shih, I. Limame, S. Krüger, C.C. Palekar, A. Koulas-Simos, D. Brunner, S. Reitzenstein, Appl. Phys. Lett., **122** (15), 151111 (2023). DOI: 10.1063/5.0143236
[10] Y.-R. Nowicki-Bringuier, J. Claudon, C. Böckler, S. Reitzenstein, M. Kamp, A. Morand, A. Forchel, J.M. Gérard. Opt. Express, **15** (25), 17291 (2007). DOI: 10.1364/oe.15.017291
[11] V.N. Astratov, S. Yang, S. Lam, B.D. Jones, D. Sanvitto, D.M. Whittaker, A.M. Fox, M.S. Skolnick, A. Tahraoui, P.W. Fry, M. Hopkinson, Appl. Phys. Lett., **91** (7), 071115 (2007). DOI: 10.1063/1.2771373
[12] B.D. Jones, M. Oxborrow, V.N. Astratov, M. Hopkinson, A. Tahraoui, M.S. Skolnick, A.M. Fox, Opt. Express, **18** (21), 22578 (2010). DOI: 10.1364/oe.18.022578
[13] F. Albert, T. Braun, T. Heindel, C. Schneider, S. Reitzenstein, S. Höfling, L. Worschech, A. Forchel, Appl. Phys. Lett., **97** (10), 101108 (2010). DOI: 10.1063/1.3488807
[14] A. Koulas-Simos, J. Buchgeister, M.L. Drechsler, T. Zhang, K. Laiho, G. Sinatkas, J. Xu, F. Lohof, Q. Kan, R.K. Zhang, F. Jahnke, C. Gies, W.W. Chow, C.-Z. Ning, S. Reitzenstein, Laser Photon. Rev., **16** (9), 2200086 (2022). DOI: 10.1002/lpor.202200086
[15] P. Jaffrennou, J. Claudon, M. Bazin, N.S. Malik, S. Reitzenstein, L. Worschech, M. Kamp, A. Forchel, J.-M. Gérard, Appl. Phys. Lett., **96** (7), 071103 (2010). DOI: 10.1063/1.3315869
[16] J.-M. Lourtioz, H. Benisty, V. Berger, J.-M. Gérard, D. Maystre, A. Tchelnokov, *Photonic crystals. Towards nanoscale photonic devices*, 2nd ed. (Springer-Verlag, Berlin, 2008).

[17] A. Babichev, I. Makhov, N. Kryzhanovskaya, A. Blokhin, Y. Zadiranov, Y. Salii, M. Kulagina, M. Bobrov, A. Vasil'ev, S. Blokhin, N. Maleev, M. Tchernycheva, L. Karachinsky, I. Novikov, A. Egorov, IEEE J. Sel. Top. Quantum Electron., **31** (5), 1900208 (2025). DOI: 10.1109/jstqe.2024.3494245
[18] I. Limame, C.-W. Shih, A. Koulas-Simos, J. Pietsch, L.J. Roche, M. Plattner, A. Koltchanov, S. Rodt, S. Reitzenstein, Opt. Express, **32** (18), 31819 (2024). DOI: 10.1364/oe.529679

Translated by J.Savelyeva